ELSEVIER

Polymer 43 (2002) 4915–4922

polymer

www.elsevier.com/locate/polymer

Structure and property studies of poly(trimethylene terephthalate) high-speed melt spun fibers

Gang Wu[a,*], Hongwei Li[a], Yiqun Wu[a], John A. Cuculo[b]

[a]College of Materials Science and Engineering, Beijing University of Chemical Technology, Box 002, Beijing 100029, People's Republic of China
[b]Fiber and Polymer Science Program, College of Textiles, North Carolina State University, Raleigh, NC 27695-8301, USA

Received 3 December 2001; received in revised form 26 April 2002; accepted 2 May 2002

Abstract

Poly(trimethylene terephthalate) has been melt spun at various take-up velocities from 0.5 to 8 km/min to prepare fiber samples. The effect of take-up velocity on the structure and properties of as-spun fibers has been characterized through measurements of birefringence, density, wide-angle X-ray scattering, DSC melting behavior, tensile properties and boiling water shrinkage (BWS). The birefringence exhibits a maximum at take-up velocities between 3 and 4 km/min. The fiber samples spun at the lower take-up speeds have essentially amorphous structures, while the filaments prepared at a velocity range higher than 4 km/min all possess an obvious crystalline structure. With increasing take-up speed, a steady improvement in tensile strength, elongation to break, and BWS is found, whereas the initial modulus remains almost constant within the measurement error, over the entire take-up speed range between 0.5 and 8 km/min. © 2002 Elsevier Science Ltd. All rights reserved.

Keywords: Poly(trimethylene terephthalate); High-speed melt spinning; Structure

1. Introduction

The utilization of linear aromatic polyesters such as poly(ethylene terephthalate) (PET) and poly(butylene terephthalate) (PBT) in the field of engineering thermoplastics and in the fiber industry is well known and widespread. In comparison to these traditional products, poly(trimethylene terephthalate) (PTT) with three methylene groups in the glycol repeating unit is a recent attention-getting polyester even though it was first polymerized by Whinfield and Dickson in 1940s [1]. PTT remained an obscure polymer for many years due to its relatively high cost. The situation has changed. The polymer is now being synthesized via a more economical process [2]. PTT offers several unique properties such as its force-elongation behavior, resilience and dyeing properties. With its outstanding elastic recovery and dyeing ability, PTT is predicted to be a promising candidate in carpet and other textile fiber applications.

Several PTT structure and properties studies have been reported [3–10]. A comparison of the vibrational spectra of PTT, PET and PBT was performed by Ward and Wilding [3]. It was found that the differences between the spectra of these polymers could be satisfactorily explained by the conformation variation in their respective molecular chains. The crystal structure of PTT was determined by several researchers for various samples prepared under different conditions [4–7], and was summarized by Yang et al. [7]. Only one crystalline form has been reported and the unit cell was found to be triclinic. The recently reported unit cell parameters for a melt crystallized PTT sample are $a = 0.46(3)$ nm, $b = 0.61(2)$ nm, $c = 1.86(1)$ nm (fiber axis), $\alpha = 97.5°$, $\beta = 92.1°$, $\gamma = 111°$, with the crystalline density of 1.40 g/cm^3 [6] and amorphous density of 1.299 g/cm^3 [8]. The flexible part consists of a three methylene group sequence with an energetically favored *trans–gauche–gauche–trans* conformation [4]. A detailed thermal analysis of semicrystalline PTT samples has also been made [9], where the glass transition temperature and typical onset temperature of the melting endotherm were reported to be 331 and 489 K, respectively. For 100% crystalline PTT, the heat of fusion is estimated to be 30 ± 2 kJ/mol [9]. The isothermal crystallization kinetics of PTT has been investigated by means of DSC and polarized light microscopy [10]. It was found that the average value of the Avrami exponent is about 2.8, and the work of chain-folding in the PTT crystalline phase is close to that of PBT

---

* Corresponding author.
E-mail address: gangwubuct@sina.com (G. Wu).

0032-3861/01/$ - see front matter © 2002 Elsevier Science Ltd. All rights reserved.
PII: S0032-3861(02)00306-3

but considerably lower than that of PET, indicating that PTT and PBT are more flexible than PET.

In addition to these studies of the structural features of PTT, there has been a few experimental studies of PTT spun fibers published in 1990s. Traub et al. reported the effect of stretch ratio on the mechanical properties of drawn PTT fibers [11]. Chuah et al. investigated the thermal stability and the melt viscosity of fiber grade PTT polymer at various shear rates and compared the resiliency, stain resistance and dyeing behaviors of the resultant PTT yarn with those of PET, polypropylene and nylon filaments [2,12]. Brown and Chuah [13] and Grebowicz et al. [8] conducted melt spinning studies of PTT at relatively lower take-up velocities (≤ 5 km/min) and reported on the resulting structure and property variations. More recently, Wu et al. reported their in situ studies of structure development in PTT fibers during different drawing processing via simultaneous synchrotron SAXS and wide-angle X-ray scattering (WAXS) measurements. A model of the phase and morphology transformation of PTT fibers was proposed [14,15].

In this article, melt spinning of PTT fiber was done over an extremely wide take-up speed range between 0.5 and 8 km/min. The effect of spinning velocity on the structure and physical properties of the as-spun PTT fiber was studied.

2. Experimental

2.1. Materials

PTT polymer produced by condensation polymerization was used in this investigation to prepare all of the fiber samples. Intrinsic viscosity of polymer chip measured in a 60/40 (wt%) mixture of phenol and tetrachloroethane is 0.92 dl/g. The PTT chips were dried in a vacuum oven at 140 °C and absolute pressure of 0.1 mmHg for 16 h before melt spinning.

2.2. Fiber spinning

Polymer chips were processed in an extruder with a screw diameter of 25 mm and a length to diameter ratio of 25. A round single-hole spinneret having 0.6 mm diameter was used to produce approximately 5 denier as-spun filament. Spinning temperature was maintained around 245 °C and a spinline length of 4.4 m, distance between the spinneret face and take-up godet, was used in the spinning process. No cross-flow or radial quench chamber was used. After passing through the atmospheric medium, the filament was collected on a godet at speeds varying from 0.5 to 8 km/min.

2.3. Measurements

Density of the fiber samples was measured following ASTM D1505-68. The density gradient column consisted of aqueous sodium bromine (NaBr) maintained at 23 ± 0.1 °C. An average value based on three tests per sample was reported. The volume crystallinity was calculated from density values, using the following equation

$$X_\mathrm{v} = (\rho - \rho_\mathrm{a})/(\rho_\mathrm{c} - \rho_\mathrm{a}) \tag{1}$$

where ρ is the density of the fiber samples, and ρ_c and ρ_a, the densities of the crystalline and amorphous phases, respectively. In accord with the literature, values of 1.40 and 1.299 g/cm^3 were used for ρ_c and ρ_a, respectively [6,8].

Fiber denier was determined by the vibroscope method in accordance with ASTM D1577. The following relation was used to calculate the linear density of the fiber samples indicated in g/cm

$$\mathrm{g/cm} = t/(4L^2f^2) \tag{2}$$

where t is the fiber tension, L, the effective fiber length, and f is the fundamental resonant frequency.

Birefringence measurements were made with a Leitz 20-order tilting compensator mounted in a Nikon polarizing microscope. An average of 10 individual determinations was reported. The radial distribution of orientation was qualitatively evaluated through observation of the parallel polarization interference patterns using a Jena interference microscope.

Thermal analysis was performed on a Perkin–Elmer DSC-7 differential scanning calorimeter. The calibration of the apparatus for temperature and energy was made using the standard indium reference. The weights of the PTT samples were kept between 8 and 10 mg, and the thermal scan rate was 20 °C/min.

WAXS intensity curves for equatorial and azimuthal scans were measured on a Rigaku Denki-model D/max-rB X-ray diffractometer system with nickel-filtered Cu Kα radiation generated at 30 kV and 20 mA. Parallel bundles of fiber samples were positioned perpendicular to the incident beam. The scattering intensities were recorded every 0.05° from equatorial scans in the range 4–40° and every 1.0° for the azimuthal scans from −90 to 90°, where the meridian was designated as 0°. The measurement of two-dimensional WAXS patterns was carried out with the diffractometer set at 40 kV and 36 mA. The data were obtained on a Fuji Imaging plate system (3000 × 3000 pixel resolution). A sample-plate distance of 127.3 mm and an exposure time of 20 min were used.

Mechanical properties of as-spun PTT fibers were measured on an Instron Model 1122 tensile tester at room temperature. All tests were performed using a gage length of 25.4 mm and a constant cross-head speed of 20 mm/min. An average of 10 individual tensile determinations was reported for each sample.

Boiling water shrinkage (BWS) was tested following ASTM D2102-79. Initial length of the fibers was measured under a pretension of 0.05 g/d. Fiber samples were immersed in boiling water at 100 °C for 5 min. After free shrinkage occurred, the samples were removed from the bath and the final length was measured. Shrinkage was then calculated using the following formula

$$\text{Shrinkage} = [(L_i - L_f)/L_i] \times 100\% \tag{3}$$

where L_i and L_f are the lengths of the fiber before and after shrinkage, respectively.

3. Results and discussion

3.1. Structure development of fiber sample

The structural development of the PTT as-spun fibers with increasing take-up velocities was followed by measurement of the birefringence and density. The results are shown in Fig. 1. The birefringence values of the fiber samples obtained over the entire range of take-up speeds are correspondingly lower than those of PET and PBT melt spun fibers prepared under corresponding conditions. For PTT, the birefringence values vary from ca. 0.008 to 0.06 in the take-up velocity covered. Comparable values for typically spun PET and PBT filaments change at a higher level from 0.01 to 0.11 in the former case and from 0.10 to 0.15 for the latter [16,17]. As shown in Fig. 1, with increasing take-up velocity from 0.5 to 3.5 km/min, birefringence increases rapidly from $\Delta n = 0.008$ to 0.06 implying that an intensive development of molecular orientation occurs in the velocity range below 3.5 km/min. After passing through a maximum of ca. 0.06 at 3.5 km/min, the birefringence value decreases slightly and then finally remains constant at ca. 0.052 with increasing take-up speed. A similar phenomenon has been observed for PET and poly(L-lactic acid) as-spun products at high spinning velocities [16,18]. This has been attributed to the birefringence distribution in cross-section of as-spun fiber wound at high speeds or the well-known skin-core double structure formed in the high-speed spun fibers [18,19]. Fig. 2 shows the parallel polarization interference patterns of the fiber samples wound at 3 and 6 km/min, respectively. It is quite evident that fiber spun at 3 km/min reveals a uniform radial structure. While the fiber spun at 6 km/min shows a skin-core structure variation, with birefringence at the fiber core being relatively lower. These results indicate that a radial differentiation of structure is also present in the PTT filaments that are spun at speeds above ca. 3.5 km/min. The optical measurements in this study, including both birefringence values and their trend with the increased speed, are consistent with Grebowicz's results although take-up velocities were limited to 5 km/min in their study [8]. In contrast, Wu et al. reported that the birefringence is roughly the same for PTT fibers spun at speeds between 1.5 and 3 km/min, and the existence of the birefringence plateau has been attributed to a rigid amorphous phase [15]. Such a phenomenon, however, was not observed in this study.

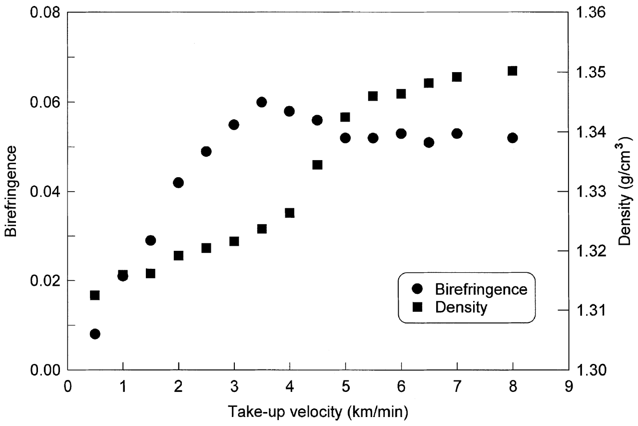

Fig. 1. Birefringence and density of as-spun PTT fibers as a function of take-up velocity.

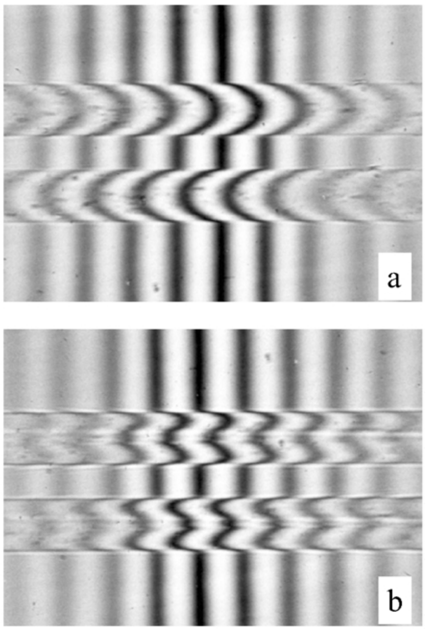

Fig. 2. Parallel polarization interference patterns of PTT fibers spun at (a) 3 km/min and (b) 6 km/min.

Density data as a function of take-up velocity are also presented in Fig. 1. The densities rise from 1.31 to 1.35 g/cm^3 in the take-up velocity range. The phenomenon can be explained that the molecular chains in PTT fiber samples oriented better along the drawing direction and the structure became more compact, even some chain segments were packed into crystal lattice, resulting in the increase of density. It is worth noting that the density increases more rapidly when the spinning speed is in the range 3.5–5.5 km/min. It has been reported that the degree of crystallinity (or density) in the as-spun fiber is determined by the product of crystallization time and crystallization rate, for a given level of orientation [20]. Increasing the take-up velocity tends to increase the threadline tension and may increase the crystallization rate through a higher level of orientation, but the crystallization time is always decreasing. In this sense, it may be assumed that the product of crystallization rate and crystallization time in the velocity range 3.5–5.5 km/min increases more rapidly than does in other ranges, resulting a rapidly increased density as presented in Fig. 1.

Fig. 3 shows the 2D WAXS photographs of three PTT as-spun fibers, which were prepared at the take-up speeds of 1, 4, and 8 km/min, respectively. As seen this figure, sample (a) shows a diffuse amorphous halo typical of PTT fibers spun at low speeds. At an intermediate level of take-up speed, i.e. 4 km/min, the indication of some developed crystalline materials is evident. This result corresponds well to the relatively high density observed at this speed. The diffraction arcs became more distinct and stronger in the case of sample (c), indicating that the crystallinity of the fiber sample produced at the ultrahigh speed is much more fully developed than those of fibers produced at relatively low speeds. The equatorial WAXS traces of PTT fibers over the entire take-up velocities are given in Fig. 4. Only broad unresolved curves with the maximum near $2\theta = 22°$ can be observed when the as-spun fibers were prepared at speeds below 4.0 km/min. The first indication of very poorly developed crystalline material is visible in the trace of the fiber prepared at 4.0 km/min. For the cases ranging from 4.5 to 8 km/min, a fairly well-resolved pattern can be observed and only one diffraction peak centers at ca. $2\theta = 16°$. It may also be observed that such a peak become more intensive and narrower with increasing spinning speed, indicating that the crystals in the fibers wound at high velocities are more perfect or having a larger size in the direction perpendicular to the crystal plane involved.

It has been reported that a polymorph phenomenon has been observed in several linear aromatic polyesters. For example, the existence of two crystal modifications, i.e. α and β forms in PBT and poly(ethylene-2,6-naphthalate) (PEN) filaments spun at high take-up velocity have been observed with WAXS measurements [17,21,22]. In comparison with PBT and PEN, diffraction peaks of crystallized PTT fibers spun at the speeds above 4.0 km/min seem to change systematically in their shape and maintain the same peak position (Fig. 4) indicating that only one crystal form exists over the experimental range. In terms of the Bragg equation and the crystalline reflection peak appearing in the equatorial scan at $2\theta = 16.0°$, the corresponding interplanar spacing d evaluated is 0.554 nm. The reflection index is then assigned to (010) planes. This reflection has an interplanar distance of 0.568 nm and was found to be the strongest one among the equatorial reflections of PTT oriented materials [4,6,15].

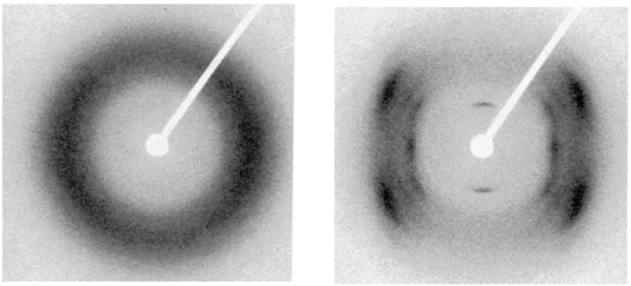

(a) 1 km/min **(b) 4 km/min**

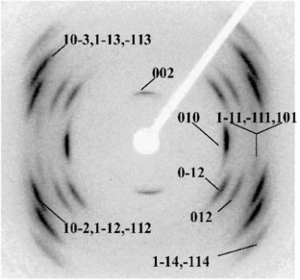

(c) 8 km/min

Fig. 3. 2D WAXS photographs of as-spun PTT fibers taken up at the indicated velocity.

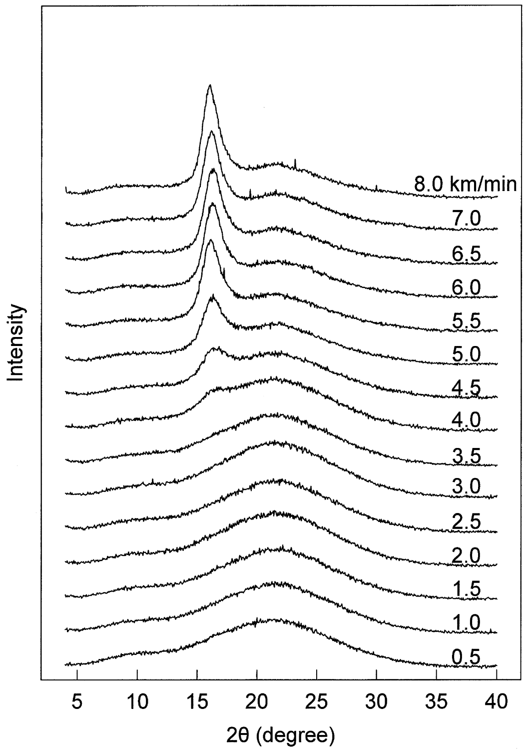

Fig. 4. Equatorial X-ray scattering profiles of as-spun PTT fibers taken up at the indicated velocity.

It is known that the measurement of the orientation index related to the intensity distribution in an azimuthal scan of a meridional $(00l)$ diffraction arc is a convenient method to evaluate the degree of alignment of the molecular chains taken to be coincident with the c-axis [23]. By performing WAXS azimuthal scans from -90 to 90° with 2θ fixed at 9.5°, the crystalline orientation index Π in various PTT fiber samples was determined using Eq. (4)

$$\Pi = (180° - H)/180° \tag{4}$$

where H is the half-width of the intensity curve along the azimuth of the (002) reflection.

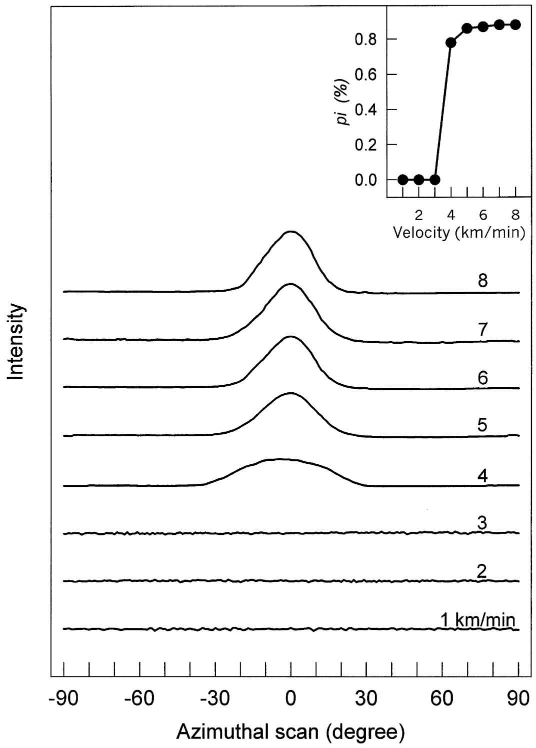

Fig. 5. Azimuthal X-ray scattering profiles of as-spun PTT fibers taken up at the indicated velocity.

Fig. 5 shows the azimuthal X-ray scattering profiles of samples wound at the indicated take-up speeds. The half-width *H* of (002) reflection was then determined for eight such samples and the index *Π* is also plotted against the take-up velocity in Fig. 5. The crystal orientation index is shown already at a high level at 4 km/min fibers and increases slightly with increasing take-up velocity. A very high and nearly saturated *Π* value is obtained in the velocity range 4–8 km/min.

3.2. Thermal behavior

Normalized DSC thermograms of these PTT fiber samples prepared at various take-up velocities are presented in Fig. 6. With increasing spinning speed, the DSC traces show an obvious change in their respective shapes and peak positions. The glass transition temperature (T_g) remains essentially constant at ca. 53 °C up to a speed of 5 km/min. For the as-spun fibers wound at lower speeds, the glass transition is followed by the cold crystallization exotherm, and following that a melting endotherm appears. The cold crystallization temperature (T_c) and melting temperature (T_m) of as-spun fiber samples are plotted against the take-up speed in Fig. 7. The position of the cold crystallization peak shifts to lower temperatures with increasing velocity. This phenomenon is very similar to that observed in the PET melt spinning process [24]. As the take-up velocity increases, the noncrystalline molecules are increasingly oriented before the initial crystallization, allowing cold crystallization to occur easier and shifting the peak to lower temperatures. In this view, the breadth of the cold crystallization peak may reflect the orientation distribution in the noncrystalline regions of these highly oriented fibers prior to the DSC scan.

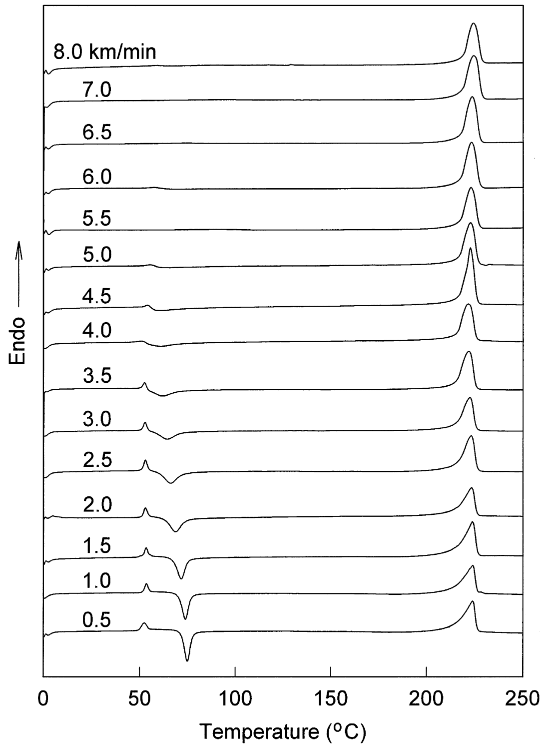

Fig. 6. DSC scans of as-spun PTT fibers taken up at the indicated velocity.

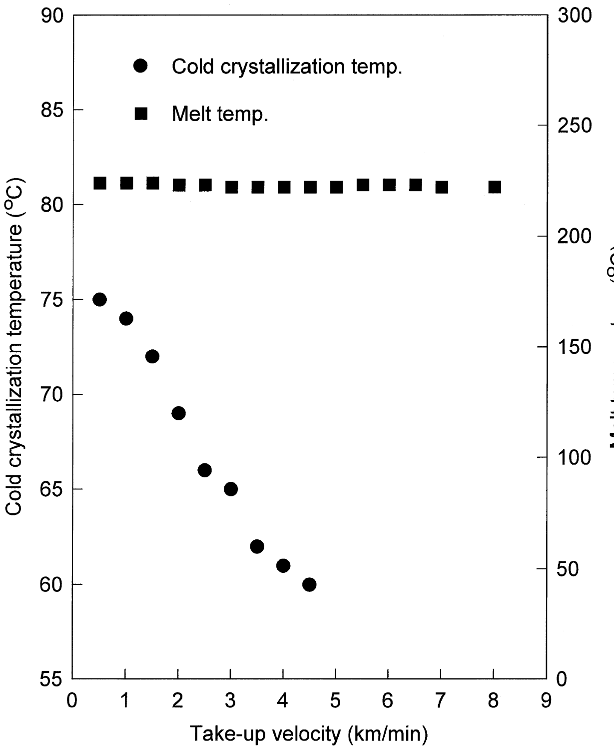

Fig. 7. Cold crystallization temperature and melting temperature as a function of take-up velocity.

The melting endothermic peak is observed near ca. 220 °C for all fiber samples. This is similar to the behavior of high-speed melt spun PET fibers but different from the PEN fibers. In the case of the high-speed melt spinning of PEN, the melting temperature of fiber samples is found to increase obviously with increasing take-up speed as a result of increasing crystalline perfection with increasing spinning speed [25,26]. Detailed analysis of this difference and related problems is planned for future studies. Further, it is also observed that the shape of the melting peaks for samples prepared at high take-up speeds 6–8 km/min is different from that of the samples spun at 0.5–2 km/min (Fig. 6). The melting endotherms of the low speed spun fibers exhibit broader and less symmetrical peaks. This may suggests an increase in the variety of crystalline components. In other words, a wider distribution in crystal sizes and crystalline perfection may exist in these low speed spun samples, because a quick cold crystallization occurred during the heat scan. Therefore, such a broader and unsymmetrical endothermic peak may be attributed to the overlap of numerous melting processes.

Furthermore, it was found that the area under the cold crystallization peak is usually smaller than that of the melting peak for the samples wound at lower speeds indicating that such fiber samples contained more or less crystalline structure before the DSC scan took place. It is known that the difference between the area under the cold crystallization peak and that of the melting peak is directly proportional to the degree of crystallinity in a sample before the thermal scan and the crystallinity, X_c, could be calculated by the application of the following relation [27]

$$X_c = (\Delta H_m - \Delta H_c)/\Delta H^0 \qquad (5)$$

where ΔH^0 is the fusion heat of 100% crystalline PTT and ΔH_c and ΔH_m are the exotherm of cold crystallization and the crystalline heat of fusion, respectively. The crystallinity thus obtained and the volume crystallinity calculated from density data (Fig. 1) as a function of take-up velocity are shown in Fig. 8. The results indicate that the as-spun PTT fibers prepared at lower speeds already contain certain amount of crystalline structure, although the crystals may be small and imperfect and then are difficult to be detected in the X-ray diffraction patterns. From Figs. 6 and 8, it is obvious that the fraction of such crystalline structure increases with increasing take-up speed, resulting in the reduction of the material that crystallizes during the subsequent DSC scan process and eventual disappearance of the cold crystallization peak at higher winding velocities. At speeds above 5 km/min, as shown in Fig. 6, only the melting exotherm is observed.

3.3. Physical properties of fiber samples

Fig. 9 shows typical stress–strain curves for as-spun PTT fiber samples as a function of take-up velocity. Three fibers prepared at lower velocities (0.5, 2, and 4 km/min) exhibit an obvious yield point, where the stress reaches a plateau region as the elongation increases. As expected, the two fiber samples wound, respectively, at 6 and 8 km/min displayed a high tenacity and low breaking elongation.

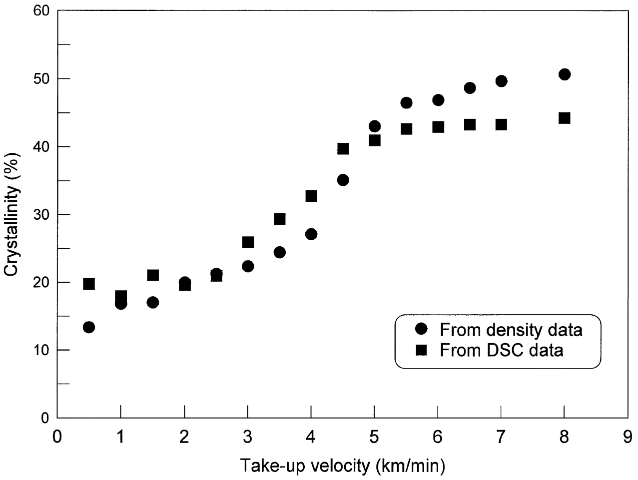

Fig. 8. Crystallinity of as-spun PTT fibers as a function of take-up velocity.

As shown in Fig. 10, the tenacity and initial modulus of as-spun PTT fiber samples as a function of take-up velocity are presented. The error in the determination of mechanical properties was about ±15%, and has been indicated in this figure. When increasing spinning speed from 0.5 to 4 km/min, the tenacity of PTT fibers increases rapidly from 0.7 to 2.8 g/d. But the tenacity levels off in the range 5–8 km/min, suggesting that highly oriented molecular chains have been formed in the as-spun products and the level of orientation has reached a saturated state as shown in Fig. 1. The maximum tenacity value obtained in as-spun PTT fibers is ca. 3.4 g/d, which is lower than that of as-spun PET fiber prepared at the same speed range where the typical tenacity is about 4 g/d [16]. In contrast to the variation of tenacity, the initial modulus shows little or no dependence on the spinning speed over the entire experimental range and

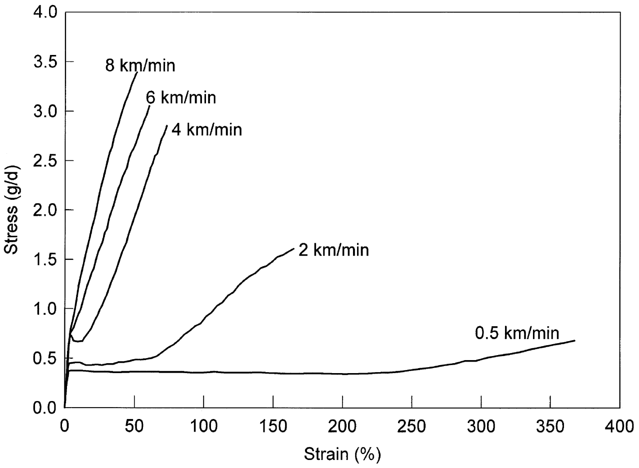

Fig. 9. Stress–strain curves of the as-spun PTT fibers prepared at different take-up velocities.

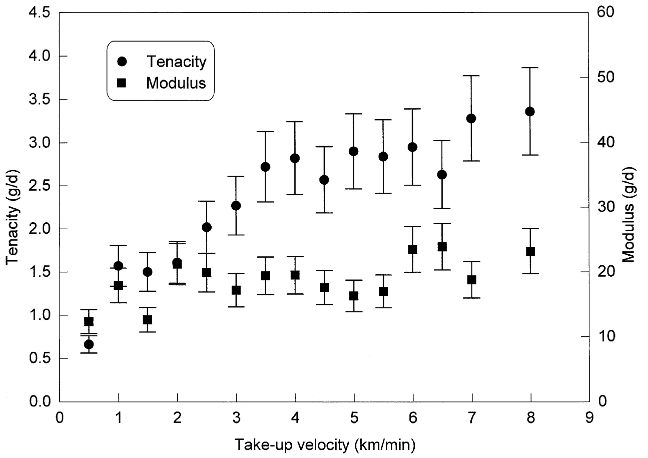

Fig. 10. Tenacity and initial modulus of as-spun PTT fibers as a function of take-up velocity.

remains at ca. 20 g/d for all samples. This seems to be somewhat different from the behavior of other homologous polyesters, such as PET and PBT. When PET and PBT fibers are prepared over a wide range of take-up speed, the modulus increased greatly as the spinning speed is increased [16,17]. In the case of as-spun PTT fibers, however, it appears that the results of initial modulus cannot be simply explained using structure parameters such as molecular orientation and degree of crystallinity. It has been reported in a previous study that the initial modulus of PTT fibers shows no dependence on the draw ratio. This phenomenon was explained on the basis of low crystallite modulus, which depends on its *trans–gauche–gauche–trans* conformation of the methylene segment [4]. The Young's modulus of the as-spun fiber produced at lower speeds may be controlled mainly by the modulus of the amorphous areas that is relatively low. With increasing take-up speeds, the oriented crystalline structures will form and they usually play a more and more important role in improving the modulus of the bulk fibers. With PET which maintains a nearly planar zigzag conformation in the crystalline lattice and then has a high crystallite modulus of ca. 108 GPa [28], it is expected that a gradually increasing fiber modulus will be achieved at higher speeds. In the case of PTT, however, the crystalline modulus has been reported to be only 2.59 GPa, and the difference between the crystalline modulus and that of the amorphous phase is small or negligible [29]. Consequently, the increased crystalline areas may not improve the modulus of bulk fiber significantly.

The breaking elongation of as-spun PTT fiber samples is plotted against the take-up speed in Fig. 11. The elongation of as-spun fiber prepared at 0.5 km/min reaches a value of 370% and then decreases gradually up to 8 km/min, where the value has dropped down to about 50%. BWS of the as-spun fibers as a function of take-up velocity is also shown in Fig. 11. The shrinkage value for fiber spun at 0.5 km/min is relatively low because of its isotropic structure. A significantly increased shrinkage exhibited in the take-up speed range from 1 to 2 km/min is caused by a disorientation process occurring in the oriented amorphous phase. The shrinkage decreases gradually as the speed exceeds 2 km/min, and then levels off and keeps constant of ca. 15% in the range 5–8 km/min. This reduction in shrinkage is attributed to the gradually developed crystalline structure, i.e. that the molecular chains pack more regularly and the crystals become more perfect at higher speed. This rationalization is in agreement with the results revealed by WAXS and DSC patterns (Figs. 4 and 6).

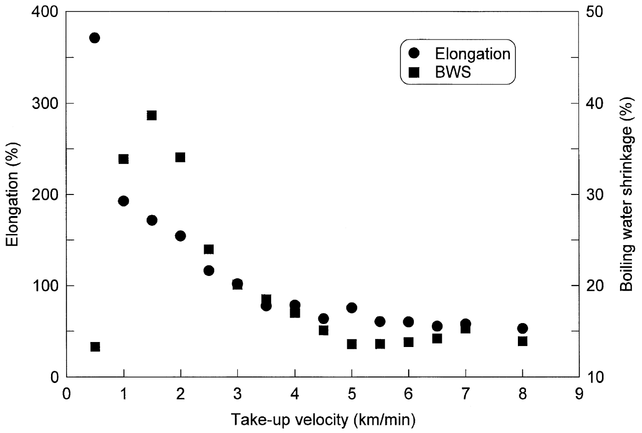

Fig. 11. Plots of breaking elongation and BWS vs. take-up velocity.

4. Conclusions

Melt spinning of PTT was carried out at various take-up velocities, up to a high speed of 8 km/min. The effect of take-up velocity on structure and physical properties of as-spun fibers was studied. Fiber samples prepared at various winding speeds exhibit quite different physical structures. Generally, high spinning speed induces a high stress along the spinline, resulting in gradual increases in molecular orientation, degree of crystallinity and physical properties. Such improvements in structure and properties are more significant in the lower velocity range from 0.5 to 4 km/min and tend to level off in the range 5–8 km/min, indicating the saturated state of molecular orientation in this higher velocity range. Furthermore, with the orientation and crystallinity increasing, as-spun PTT fibers also present fair physical properties. The highest tenacity value obtained in as-spun PTT fibers is 3.4 g/d and the initial modulus remains constant of ca. 20 g/d over the entire spinning speed range. The breaking elongation and BWS of fiber samples can be diminished to ca. 50 and 15%, respectively. These values were obtained for take-up velocities of 5–8 km/min.

Acknowledgments

The support from National Natural Science Foundation of China (grant no. 59873003) and China Petroleum and

Chemical Corporation (SINOPEC, X599017) was gratefully appreciated.

References

[1] Whinfield JR, Dickson JT. Br Patent 578,079; 1941. US Patent 2,465,319; 1949.
[2] Chuah HH. Chem Fibers Int 1996;46:424.
[3] Ward IM, Wilding MA. Polymer 1977;18:327.
[4] Poulin-Dandurand S, Perez S, Revol JF, Brisse F. Polymer 1979;20:419.
[5] Desborough IJ, Hall IH, Neisser JZ. Polymer 1979;20:545.
[6] Wang B, Li CY, Hanzlicek J, Cheng SZD, Geil PH, Grebowicz J, Ho RM. Polymer 2001;42:7171.
[7] Yang J, Sidoti G, Liu J, Geil PH, Li CY, Cheng SZD. Polymer 2001;42:7181.
[8] Grebowicz JS, Brown H, Chuah H, Olvera JM, Wasiak A, Sajkiewicz P, Ziabicki A. Polymer 2001;42:7153.
[9] Pyda M, Boller A, Grebowicz J, Chuah H, Lebedev BV, Wunderlich B. Polym Sci, Part B: Polym Phys 1998;36:2499.
[10] Huang JM, Chang FC. Polym Sci, Part B: Polym Phys 2000;38:934.
[11] Traub HL, Hirt P, Herlinger H. Chem Fibers Int 1995;45:110.
[12] Chuah HH, Brown HS, Dalton PA. Int Fiber 1995;October:50.
[13] Brown HS, Chuah HH. Chem Fibers Int 1997;47:72.
[14] Wu J, Schultz JM, Samon JM, Pangelinan AB, Chuah HH. Polymer 2001;42:7141.
[15] Wu J, Schultz JM, Samon JM, Pangelinan AB, Chuah HH. Polymer 2001;42:7161.
[16] Murase Y. Sen-I Gakkaishi 1991;47:P564.
[17] Chen S, Spruiell JE. Appl Polym Sci 1987;33:1427.
[18] Mezghani K, Spruiell JE. Polym Sci, Part B: Polym Phys 1998;36:1005.
[19] Shimizu J, Okui N, Kikutani T, Toriumi K. Sen-I Gakkaishi 1978;34:T93.
[20] Cuculo JA, Tucker PA, Chen GY. Appl Polym Sci, Appl Polym Symp 1991;47:223.
[21] Cakmak M, Kim JC. Appl Polym Sci 1997;64:729.
[22] Wu G, Liu M, Li XN, Cuculo JA. Polym Sci, Part B: Polym Phys 2000;38:1424.
[23] Alexander LE. X-ray diffraction methods in polymer science. New York: Wiley; 1969.
[24] Heuvel HM, Huisman R. Appl Polym Sci 1978;22:2229.
[25] Miyata K, Kikutani T, Okui N. Appl Polym Sci 1997;65:1415.
[26] Wu G, Li QC, Cuculo JA. Polymer 2000;41:8139.
[27] Cakmak M, Wang Y, Simhambhatla M. Polym Engng Sci 1990;30:721.
[28] Tashiro K. Prog Polym Sci 1993;18:377.
[29] Nakamae K, Nishino T, Hata K, Yokoyama F, Matsumoto T. J Soc Mater Sci: Japan 1986;35:1066.